J. metamorphic Geol., 2006, **24,** 281–295 doi:10.1111/j.1525-1314.2006.00637.x

Evolution of H_2O content in a polymetamorphic terrane: the Plattengneiss Shear Zone (Koralpe, Austria)

V. TENCZER,[1] R. POWELL[2] AND K. STÜWE[1]
[1]*Institut für Erdwissenschaften, Universität Graz, Heinrichstr. 26, A-8010 Graz, Austria (tenczer@uni-graz.at)*
[2]*School of Earth Sciences, University of Melbourne, Melbourne, Vic. 3010, Australia*

ABSTRACT The Koralpe of the Eastern European Alps experienced high-temperature/low-pressure metamorphism (~650 °C and 6.5 kbar) during the Permian and eclogite facies metamorphism (~700 °C and 14 kbar) during the Eo-Alpine (Cretaceous) metamorphic event. In the metapelitic Plattengneiss shear zone that constitutes much of the Koralpe, the second metamorphism caused only partial re-equilibration of the assemblages formed during the first metamorphism. It is shown here that the Eo-Alpine mineral assemblage, garnet + biotite + muscovite + plagioclase + quartz (with or without kyanite), formed under low water activity conditions that are consistent with the level of dehydration that occurred during the Permian event. This implies that the rocks were essentially closed-system from the peak of the Permian metamorphism through the Eo-Alpine event. The evolution of water content of the rocks is traced through time: that prograde dewatering during the Permian metamorphic event terminated at the metamorphic peak with a water content around 3–4 mol.%. The water content remained then constant and led to water-undersaturation during the subsequent Eo-Alpine metamorphism. From the water content and activity evolution a post-peak isothermal decompression path close to the solidus is inferred for the Eo-Alpine event.

Key words: polymetamorphism; Plattengneiss shear zone; Koralpe region; water content; water activity; phase diagrams.

INTRODUCTION

A widespread phenomenon in many polymetamorphic terranes is that rocks re-equilibrated only partially during all but the first metamorphic event (Francesch-helli *et al.*, 1998; Rickers *et al.*, 2001; Zeck & Whitehouse, 2002). This is a common observation in polymetamorphic terranes, even when the metamorphic temperatures during later events were higher than during earlier ones. Two arguments have traditionally been brought forward to explain this observation. The first is that high-grade metamorphism during later events was probably short-lived (Lister *et al.*, 2001) and shorter than earlier events. Diffusivities of cations in crystal lattices are extremely slow and many chemical systems require time scales of 10^7–10^8 years for their equilibration. For example, the Fe–Mg exchange system in garnet requires several tens of million years for the equilibration of length scales of several centimetres, even at 700 °C (e.g. Stüwe & Ehlers, 1996). As a consequence, shorter metamorphic events will allow rocks to equilibrate only partially.

The second argument – and the subject of this paper – is that the rocks may have been fluid absent during all but the first metamorphic event. Given that metamorphic fluids are known to be extremely efficient agents for transport across grain boundaries it is plausible that the absence of a free fluid hinders chemical equilibration. Guiraud *et al.* (2001) have proposed that equilibrium in rocks is likely to be maintained as pressure and temperature change while there is a fluid phase present, but that continued equilibration effectively ceases when the fluid phase is used up by retrograde reaction, for example, as the rock starts to cool. Guiraud *et al.* (2001) promote this idea as the principal mechanism for the preservation of mineral assemblages from the metamorphic peak. Within this model, the water content of the rock is established at the metamorphic peak (i.e. only water structurally bound in the minerals that remains in the rock) and is maintained during all subsequent events, unless the system is open to external fluid infiltration at a late stage.

This idea is evaluated for a classic polymetamorphic terrane: the Koralpe of the Eastern Alps. The region hosts the eclogite type locality (e.g. Tenczer & Stüwe, 2003) and one of the largest shear zones of the Alps, the Plattengneiss shear zone (e.g. Kurz *et al.*, 2002; Putz *et al.*, 2006). We set out to quantify the evolution of water content and water activity of the rocks within this shear zone through time and across two metamorphic events. This information is then used to infer aspects of the metamorphic evolution of the region. In particular we suggest that the pervasive dehydration during the first metamorphic event experienced by the region in the Permian was the main reason for the

heterogeneous equilibration during the second event (referred to as 'Eo-Alpine') event in the Cretaceous. A mineral equilibria approach is followed, using calculated pseudosections appropriate to the bulk compositions of the Plattengneiss during the Permian and Eo-Alpine metamorphic events.

GEOLOGICAL OVERVIEW

The Kor/Saualpe region of the Eastern European Alps is the largest continuous region of the Alps in which amphibolite and eclogite facies metamorphic rocks from the Eo-Alpine metamorphic cycle are preserved (Frey *et al*., 1999; Oberhänsli *et al*., 2004) (Fig. 1a). The region includes mafic bodies of the type-locality eclogites that are up to hundreds of metres in length, but it is mostly made up of pelitic gneisses with garnet, mica and kyanite-bearing assemblages. The entire region experienced eclogite facies metamorphism at ~14 kbar and 700 °C during the Eo-Alpine metamorphic cycle at *c*. 90 Ma (Thöni & Jagoutz, 1992; Stüwe & Powell, 1995; Miller & Thöni, 1997; Tenczer & Stüwe, 2003). However, the pelitic precursors are older and were previously metamorphosed during the Permian. The Permian metamorphic event was dated via the age of the gabbroic precursors of the eclogites (Thöni & Jagoutz, 1992). Ages of *c*. 250 Ma are also given by garnet from pegmatites and primary coarse-grained muscovite (Morauf, 1981; Frank *et al*., 1983; Thöni & Miller, 1996; Habler & Thöni, 2001). A

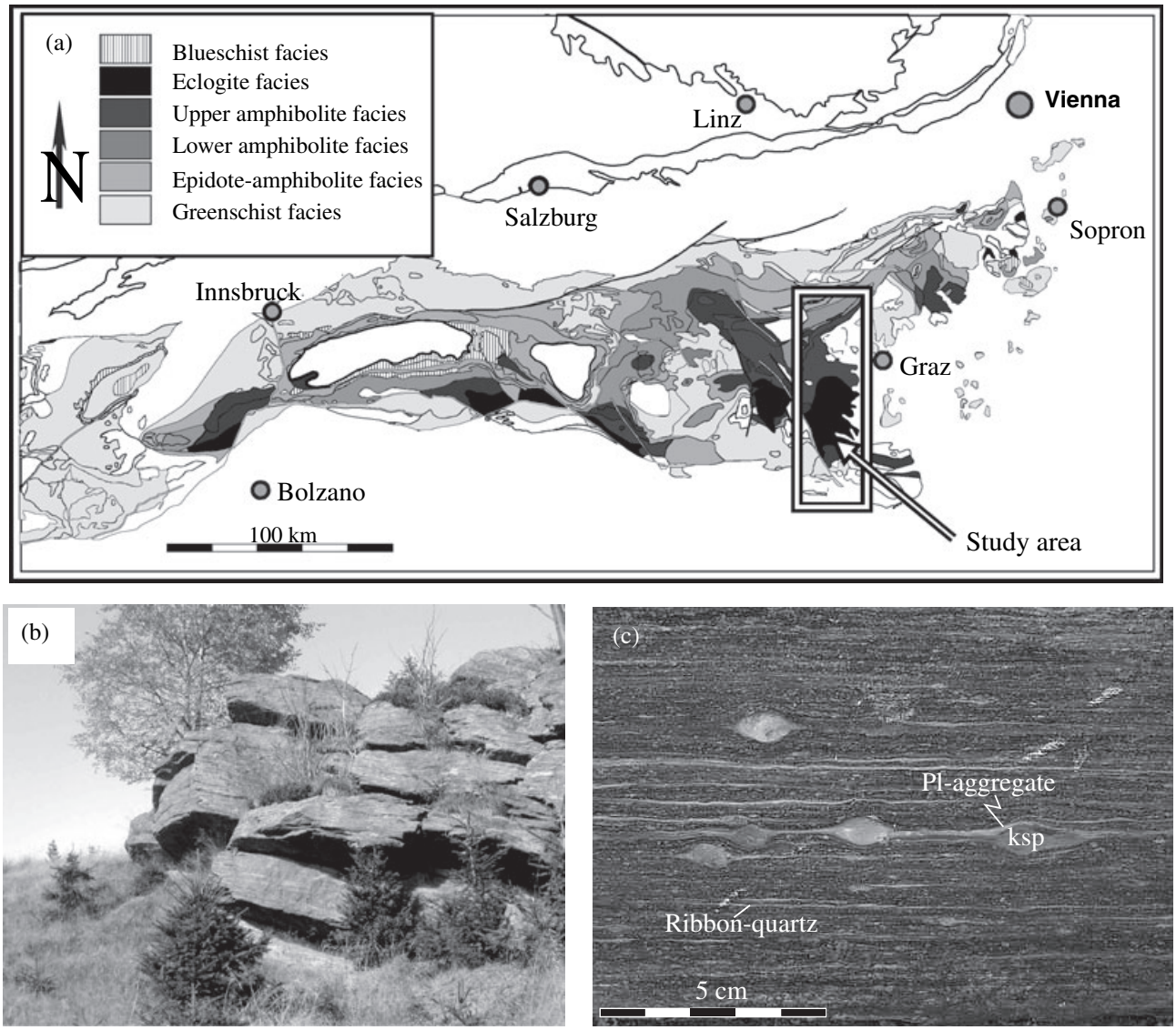

Fig. 1. Location map and field photographs of the Plattengneiss shear zone. (a) Metamorphic map of the Eastern Alps showing distribution of Eo-Alpine metamorphic grade (modified after Oberhänsli *et al*., 2004). (b) Typical outcrop of the Plattengneiss shear zone in the Koralpe. (c) Hand specimen of the Plattengneiss mylonite with sheared porphyroclasts of K-feldspar and plagioclase aggregates.

Permian age for an earlier metamorphic event affecting these rocks is therefore now considered to be well-established. The metamorphic peak conditions of this Permian event were constrained by Habler & Thöni (2001) to be ~600 °C and 4 kbar. Detailed petrographic and mineral chemical studies of the pelitic gneisses in the region were recently published by Habler & Thöni (2001), Tenczer & Stüwe (2003) and others and these studies should be referred to for further details. Despite the large abundance of Variscan ages in the areas north of the Koralpe/Saualpe region, no relics of Variscan metamorphic events are found in the entire study area. Therefore, it is assumed that the Permian event was the first metamorphic event affecting the region.

One of the most important structures in the region is the Plattengneiss shear zone. This flat-lying shear zone crops out on the eastern slope of the Koralpe, and equivalent sheared rocks occur in the Saualpe to the west (Fig. 1b). The shear zone is roughly 1 km thick and it is exposed over more than 600 km^2 (Putz *et al.*, 2006). It is characterized by a strong north–south-oriented lineation and extreme strain with individual feldspar crystals stretched out up to 1 m in length (Krohe, 1987). Because the shear zone is undoubtedly one of the major features involved in the Cretaceous stacking of the Austroalpine nappe pile (Kurz *et al.*, 2002), it has been used extensively to constrain the Eo-Alpine deformation event in both physical conditions and time.

The rocks of the Plattengneiss shear zone are very heterogeneously equilibrated during the Eo-Alpine metamorphism. This has long been the bane of geochronologists trying to constrain various metamorphic events in the region and some of the textural evidence is summarized below (see also Tenczer & Stüwe, 2003). The lack of equilibration has been interpreted in terms of both a short-lived duration of the Eo-Alpine metamorphic event and fluid absence during metamorphism. For example, Frank *et al.* (1983), Tenczer & Stüwe (2003) and others have argued that the rocks were fluid absent during the Eo-Alpine metamorphic cycle. In contrast, Stüwe (1998) and others have argued that the Eo-Alpine event was short-lived. However, of these two arguments, only the duration of the Eo-Alpine event has been studied in any detail: the total time of cooling is roughly constrained by geochronological data (Hejl, 1997; Thöni, 2002). A temperature–time evolution has been established by Neubauer *et al.* (1995) for the northern part of the region and direct cooling rate measurements have been performed by Ehlers *et al.* (1994). In contrast, the water content has not been studied for the eclogite facies metamorphism during the Eo-Alpine event. In the remainder of this paper, we will document the amount of fluid that was present during and before the Eo-Alpine metamorphic cycle and show that the rocks were initially dehydrated by Permian metamorphism.

PETROGRAPHY AND MINERAL CHEMISTRY

The Plattengneiss

The Plattengneiss is a metapelitic rock with a strong mylonitic fabric and abundant smeared-out pegmatitic intercalations that often disintegrate into individual K-feldspar augen due to the extreme strain (Fig. 1c). Its mineralogy includes garnet, biotite, muscovite, plagioclase, kyanite, K-feldspar and quartz with accessory tourmaline, apatite, zircon and oxides. Staurolite, paragonite and chlorite do occur in more hydrated equivalents of the Plattengneiss (see below), but the composition of these rocks is not discussed here. Because of the mylonitic fabric, most minerals are fine-grained, but K-feldspar forms large ductily-deformed clasts with core-mantle structures that are up to many centimetres in size. There are also plagioclase aggregates that form clasts which appear macroscopically similar to the K-feldspar clasts (Fig. 1c). Also, garnet, kyanite and muscovite fish may occur as millimetre-sized clasts and trails in a matrix that consists of dynamically recrystallized grains of quartz, plagioclase and muscovite (Fig. 2a). Kyanite is commonly present as recrystallized fine-grained aggregates that are paramorphs after andalusite/sillimanite. Habler & Thöni (2001) have shown that much of the Permian aluminosilicate is likely to have been sillimanite. However, outside the Plattengneiss shear zone paramorphs of kyanite after andalusite are up to metres in size showing remnant chiastolite crosses (see fig. 3b of Tenczer & Stüwe, 2003). Not all of the minerals listed above are likely to have been part of the same equilibrium paragenesis as is reflected in the metamorphic textures.

Because it is well-established that the two texturally discernible mineral generations belong to the Permian and the Eo-Alpine metamorphic events, we will refer to them with respect to these events in the description below. For our discussion the mineral abbreviations are: g, garnet; bi, biotite; mu, muscovite; sill, sillimanite; ky, kyanite; chl, chlorite; st, staurolite; pa, paragonite; q, quartz; pl, plagioclase; ksp, K-Feldspar; Grs, grossular; Alm, almandine; Prp, pyrope; Sps, spessartine; An, anorthite.

The Eo-Alpine garnet (g2) can be distinguished from an earlier garnet generation (g1) on the basis of metamorphic texture in thin section and mineral chemistry (see Tenczer & Stüwe, 2003 and Fig. 2b–d). Eo-Alpine garnet (g2) grew syn-deformational at high strain conditions and contain abundant inclusions of muscovite, biotite and quartz. They often form fine-grained deformed aggregates and occur as bands in the matrix, but have typically idiomorphic rims. The average compositions of g2-garnet is $X_{Grs} = 0.15$, $X_{Prp} = 0.25$, $X_{Alm} = 0.59$ and $X_{Sps} = 0.01$ (Fig. 2c, Table 1). In contrast, Permian garnet (g1) is larger in size and have few inclusions (of quartz and biotite). They occur either as separate rounded grains in the quartz-feldspar matrix or as cores overgrown by irregular Eo-Alpine garnet

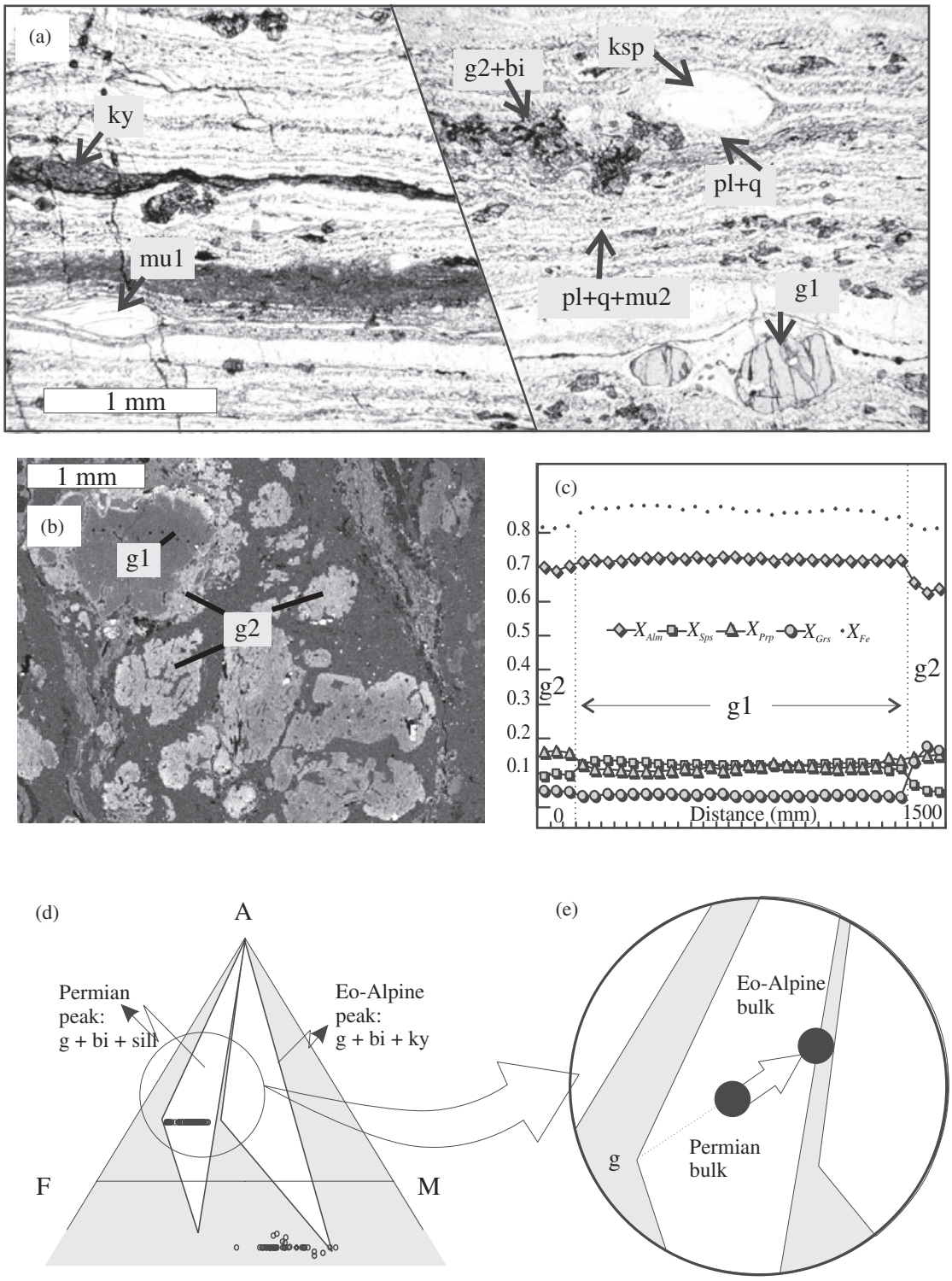

Fig. 2. Summary of the petrography of the Plattengneiss shear zone. (a) Collage of two photomicrographs from the Plattengneiss. Note two generations of garnet (g) and muscovite (mu) ('1' is part of the Permian assemblage; '2' is part of the Eo-Alpine assemblage). (b) Backscattered electron image of garnet in the Plattengneiss. Note the easily distinguished older garnet generation. (c) Compositional profile across the two-generation garnet shown in the top left corner in (b). (d) Calculated AFM-diagram (projected from mu, q and H_2O) showing the equilibrium divariant assemblage g + bi + aluminosilicate for Permian (650 °C and 6.5 kbar) and Eo-Alpine (700 °C and 14 kbar) metamorphic conditions as calculated with THERMOCALC. Also shown are the actual chemical compositions of garnet and biotite analysed from the Plattengneiss. (e) Enlargement from Fig. 2d indicating the evolution of the bulk composition from the Permian to the Eo-Alpine event in AFM.

Table 1. Summary of some mineral chemical parameters of the Plattengneiss and surrounding rocks. The top part of the table is for Permian minerals. PG is a Plattengneiss from our own data and DFG is a less deformed Disthenflasergneiss from Habler & Thöni (2001). The Eo-Alpine compositions of eight sample also used by Tenczer & Stüwe (2003) are shown in the bottom part of the table (sample numbers correspond to those by Tenczer & Stüwe, 2003).

Permian	Garnet		Biotite		Muscovite			Plagioclase	
Rock type/mineral parameter	x(g)	z(g)	x(bi)	y(bi)	x(mu)	y(mu)	z(mu)	ca(pl)	k(pl)
PG	0.88	0.05	–	–	0.4	0.8	0.028	0.22	0.01
DFG	0.86–0.89	0.05–0.06	0.57	0.37–0.38	0.53	0.885	0.02	0.33	0.01
Typical	**0.88**	**0.05**	**0.55**	**0.35**	**0.5**	**0.88**	**0.03**	**0.3**	**0.01**
Eo-Alpine	Garnet		Biotite		Muscovite			Plagioclase	
Sample no./mineral parameter	x(g)	z(g)	x(bi)	y(bi)	x(mu)	y(mu)	z(mu)	ca(pl)	k(pl)
12	0.68–0.76	0.03–0.15	0.3–0.37	0.2–0.3	0.25–0.27	0.53–0.69	0.028–0.034	0.138–0.235	0.008–0.014
13	0.66–0.69	0.03–0.01	0.32–0.37	0.34–0.48	0.21–0.25	0.62–0.65	0.025–0.033	0.144	0.006
15	0.69	0.15	0.37–0.4	0.15–0.395	0.24–0.26	0.57–0.59	0.036		
17	0.69	0.14	0.38–0.39	0.32–0.37	0.24	0.66	0.026	0.141–0.211	0.012–0.013
18	0.72–0.78	0.02–0.05	0.33–0.4	0.18–0.44	0.21–0.32	0.4–0.5	0.26–0.036	0.134	0.014
19	0.71	0.07	0.4–0.49	0.27–0.35	0.31	0.61	0.028	0.176	0.015
20	0.73–0.82	0.2–0.25	0.3–0.4	0.3–0.4	0.21–0.23	0.54–0.57	0.026–0.028	0.134	0.021
21	0.68–0.7	0.03–0.05	0.34–0.36	0.33–0.34	0.22	0.51	0.028	0.135	0.009
Typical	**0.7**	**0.1**	**0.3**	**0.25**	**0.25**	**0.55**	**0.03**	**0.13–0.14**	**0.01**

Abbreviations: For garnet: x = X_{Fe}, z = Ca/3. For biotite: x = X_{Fe}, y = X_{Al}(M2A). For muscovite: x = X_{Fe}, y = X_{Al}(M2A), z = X_{Na}. For plagioclase: ca = X_{An}, k = X_{Ksp}.

aggregates (Fig. 2b). Permian garnet shows higher Mn content and lower Ca content than Eo-Alpine garnet. Generally, Permian g1-garnet relics have average compositions of about $X_{Grs} = 0.03$, $X_{Prp} = 0.12$, $X_{Alm} = 0.72$, $X_{Sps} = 0.12$ (Fig. 2c). The muscovite grown during Eo-Alpine metamorphism (mu2) shows Si contents of about 3.1–3.2 a.p.f.u (Fig. 6c in Tenczer & Stüwe, 2003). These contents are higher than the older-generation muscovite (mu1) occurring as fish. The cores of these fish show a muscovite composition with Si = 3.02–3.1 a.p.f.u. Eo-Alpine biotite is a minor constituent and is characterized by X_{Mg} between 0.60 and 0.75 (Table 1). It mainly occurs in pressure shadows in and around garnet aggregates, but some biotite flakes do occur in the matrix. The plagioclase shows a compositional variation of $X_{An} = 0.09$–0.30 (Table 1).

K-feldspar in the Plattengneiss

A particular problem is the occurrence of large K-feldspar porphyroblasts in the Plattengneiss that are abundant and often are up to many centimetres in size (Figs 1c & 2a). In fact, it is often smeared out K-feldspar that defines the macroscopic lineation of the rock. It is not clear how much of this K-feldspar belongs either to the Permian or to the Eo-Alpine metamorphic assemblage. The high Eo-Alpine strain in the Plattengneiss mylonite makes it difficult to infer its stability (or instability) on textural grounds. Moreover, K-feldspar is always mantled by plagioclase seams and textural equilibrium with other surrounding minerals cannot be established. We therefore suggest that the majority of the K-feldspar clasts could not have been part of the Eo-Alpine assemblage. In order to test for the feasibility of K-feldspar being part of the Permian equilibrium assemblage, calculations were made on the stability of K-feldspar in muscovite and quartz-bearing assemblages for the whole-rock composition of the Plattengneiss using THERMOCALC. It is shown that the NCKFMASH divariant paragenesis garnet + biotite + muscovite + plagioclase + sillimanite + quartz + H_2O + K-feldspar produces only small amounts of K-feldspar but causes rapid consumption of muscovite for bulk compositions similar to that of the Plattengeiss. This precludes the stable coexistence of abundant K-feldspar with muscovite. This is also confirmed by White *et al.* (2001) who showed that even K_2O-rich bulk compositions produce little K-feldspar at the *P–T* conditions or water contents of our interest.

Two alternatives for the origin of K-feldspar are possible. It may either have been included in the Plattengneiss (i) as K-feldspar pebbles in the precursor sediment prior to the Permian or (ii) as remnants of pegmatites formed by partial melting during the Permian, which are abundant in the Koralpe within and outside the Plattengneiss shear zone. Here, it is suggested that the K-feldspar is of pegmatitic origin. Several observations confirm this: (i) tourmaline porphyroblasts – common constituents of the Permian pegmatites outside the Plattengneiss shear zone – are often spatially related to K-feldspar in the shear zone, even if they are not obviously within the same smeared out pegmatite. (ii) Although water-saturated melting does not produce any K-feldspar bearing reaction spaces immediately above the solidus (see phase diagrams below), 100 °C above the solidus the modal ratio of melt to K-feldspar is about 2:1. We suggest from field experience that this may correspond to the observed ratio of feldspar augen to pegmatite. (iii) There is also the circumstantial evidence that a detrital K-feldspar is likely to have been transformed into

sericite during the prograde Eo-Alpine evolution. However, we will show below that it may also be possible that some K-feldspar has grown on the prograde path of the Eo-Alpine event, but became unstable before the metamorphic peak was reached.

From these observations Tenczer & Stüwe (2003) interpreted the Eo-Alpine peak metamorphic assemblage to involve garnet + biotite + muscovite + plagioclase + quartz with or without kyanite. This mineral assemblage corresponds to maximum Eo-Alpine peak conditions of *c*. 700 °C and 14 kbar (Stüwe & Powell, 1995; Tenczer & Stüwe, 2003). The earlier Permian mineral assemblage has been interpreted to consist of garnet + biotite + muscovite + plagioclase + sillimanite + quartz (Habler & Thöni, 2001). A geochronologically well-constrained example of this assemblage from a Plattengneiss-equivalent in the Saualpe discussed in detail by Habler & Thöni (2001) formed at 249 ± 3 Ma, at conditions which they deduced to be about 600 °C and 4 kbar. This sample was used as a basis for calculations relating to the Permian metamorphic event in our pseudosection study.

The rocks surrounding the Plattengneiss

Although the Plattengneiss shear zone is the subject of this paper, the surrounding rocks have some mineralogical differences that should be discussed. In principle, the rocks surrounding the Plattengneiss shear zone are the same high-grade metamorphic metapelitic gneisses as the shear zone itself. However, they are often more hydrated indicated by the presence of staurolite, chlorite and/or paragonite. Staurolite typically occurs as inclusions or as small rims on garnet. In lower grade equivalents of the Plattengneiss staurolite has also been interpreted to occur in Permian as well as Eo-Alpine generations. Paragonite occurs as inclusions in garnet and as intergrown bundles together with muscovite. Chlorite is a typical retrograde reaction product in pressure shadows around garnet in more hydrated rocks.

BULK COMPOSITIONS

For the mineral equilibria modelling below, a bulk composition for the Plattengneiss is needed. The bulk compositions appropriate for considering the Permian and the Eo-Alpine events differ because some of the phases occur in two generations and not all phases were part of the effective bulk composition during both events. For the phase diagram calculations presented below it is therefore crucial to determine a relevant bulk composition and its robustness for modelling each of the two metamorphic events.

The estimation of the bulk composition was done with different approaches in order to test the sensitivity of the mineral assemblages in the calculated pseudosections. The first approach involved point-counting the distribution of Eo-Alpine and Permian minerals in thin section (e.g. bulk composition 'eopg1', 'permpg1' and 'inteo' in Table 2 and Fig. 3c). With the corresponding mineral chemistry and the mineral proportions an appropriate bulk composition was calculated. The second approach was based on the mineral proportions gained by point-counting and theoretically calculated mineral parameters at the relevant peak conditions done with THERMOCALC ('eopg2' and 'permpg2' in Table 2 and Fig. 3c). In a third approach we used the whole-rock chemistry, with adjustments that take account of the proportions of minerals not involved in the development of the equilibrium mineral assemblage in the specific event ('eopg3' and 'permpg3' in Table 2 and Fig. 3c). The different approaches gave comparable bulk compositions for several samples from the Plattengneiss shear zone and also the surrounding metapelitic gneisses. Here we use bulk compositions derived from the third approach (i.e. bulks 'eopg3' and 'permpg3' in Table 2), because it is easiest to compare this with previous studies (e.g. Stüwe & Powell, 1995). We therefore explain the derivation of these two bulk compositions in more detail below.

Permian bulk composition (permpg3)

The bulk composition of the Plattengneiss during the Permian event is taken to be that of the whole rock, given that no pre-Permian metamorphic minerals are present in the Plattengneiss that may not have been part of the Permian effective bulk. An appropriate adjustment is only made with respect to the big K-feldspar porphyroclasts that are presumed not to be

Table 2. Bulk compositional variation of the Plattengneiss and surrounding rocks as derived from different approaches discussed in text and for different metamorphic events. The bold printed bulks are those used in Figs 3–5. For comparison the bulk composition of the average metapelite used by White *et al.* (2001) is added (white). All bulks are also shown in Fig. 3(c).

Bulk composition	SiO_2	Al_2O_3	CaO	MgO	FeO	K_2O	Na_2O	x	y
eopg1	72.48	12.84	0.51	4.34	4.39	1.98	3.46	0.50	0.60
eopg2	71.84	12.96	1.64	3.69	4.78	1.87	3.22	0.56	0.60
eopg3	**79.85**	**8.85**	**1.51**	**2.78**	**3.03**	**1.68**	**2.30**	**0.52**	**0.60**
permpg1	68.32	15.18	3.03	1.97	7.32	1.44	2.74	0.79	0.62
permpg2	69.34	13.36	1.68	3.79	7.04	1.88	2.92	0.65	0.55
permpg3	**76.93**	**10.16**	**1.47**	**2.87**	**4.50**	**1.94**	**2.14**	**0.61**	**0.57**
inteo	69.11	16.27	1.26	3.52	4.79	2.04	3.00	0.58	0.66
white	70.00	11.55	0.37	4.70	8.95	3.70	0.73	0.65	0.45

Abbreviations: x = Fe/(Fe + Mg), y = Al/(Al + Fe + Mg).

a part of the meta-pelitic bulk composition (see above). For the whole-rock composition, the XRF analysis of sample 48/92 was used, a typical Plattengneiss that was discussed at length by Stüwe & Powell (1995) (Table 3, lines a and b). There are several Vol.% of K-feldspar (with an average composition of K/(K + Na) = 0.9) in this sample, with an unknown proportion being involved in the Permian bulk composition. We have chosen to remove 2 Vol.% of K-feldspar from the bulk composition, and discuss below the consequence of varying this amount. An appropriate subtraction of K_2O, Na_2O, Al_2O_3 and SiO_2 was done to account for this K-feldspar not being a part of the Permian bulk composition (Table 3, line c). The calculations for this bulk composition were undertaken with H_2O in excess, on the assumption that the Permian event was the first metamorphic event affecting the rocks and thus that water-saturated conditions were maintained during the prograde history.

Eo-Alpine bulk composition (eopg3)

The bulk composition of the Plattengneiss during the Eo-Alpine metamorphic event is not as easily determined. The Permian mineral relics, such as garnet and mica fish, did apparently not take part in the equilibration during the Eo-Alpine part of the metamorphic evolution. This means that the Eo-Alpine bulk composition differs from the Permian bulk composition to some extent. In order to derive a bulk composition for the Eo-Alpine that can be compared with the Permian bulk composition, proportions of phases are subtracted from the Permian bulk discussed above (Fig. 2e). The mineral modes of the Plattengneiss during the Permian are unknown. Thus, the calculated modal composition of the rock at the Permian metamorphic peak conditions is used. This is then adjusted for the phases (garnet and muscovite) that did not take part in the subsequent Eo-Alpine evolution.

Habler & Thöni (2001) estimated metamorphic peak conditions for the Permian event at ~600 °C and 4 kbar for the assemblage g + bi + mu + sill + pl + q + H_2O using GEO-CALC (Brown *et al.*, 1988) and the thermodynamic data set of Berman (1988). In order to ensure internal consistency of the calculations, these conditions were re-estimated using the published mineral compositions for this rock (Table 1 of Habler & Thöni, 2001) and THERMOCALC 3.23 (Powell *et al.*, 1998 and upgrades). These calculations give average pressures of 6.5 kbar at 650 °C for the Permian metamorphic peak (Table 4). The peak temperature of 650 °C was chosen for the average pressure calculations because it is the lowest temperature consistent with the stability range of the Permian peak assemblage on the pseudosection discussed below (Fig. 3). These metamorphic conditions and the Permian bulk composition shown in Table 3, line c, was then used to calculate the mineral modes in the trivariant field g + bi + mu + sill (+ pl + q + H_2O) at the Permian metamorphic peak. These modes and the corresponding mineral compositions are shown in Table 3, line d. Finally, the entire Permian garnet mode and half of the Permian muscovite listed in Table 3, line d were subtracted from the bulk so that they are not part of the equilibration at Eo-Alpine times.

The resulting bulk composition is shown in Table 3 ('eopg3' in line e) and is appropriate for the phase diagram calculations relating to the Eo-Alpine metamorphic event. A test of this approach to derive the Eo-Alpine bulk composition can be made by a comparison of the X_{Fe} of the bulk with that of the Permian biotite. Our model predicts that Eo-Alpine bulk and Permian biotite should have the same X_{Fe}

Table 3. Derivation of bulk compositions for the Plattengneiss to consider the Permian and the Eo-Alpine events based on sample 48/92 of Stüwe & Powell (1995).

(a) Weight per cent of sample 48/92 in NCKFMAS (from Stüwe & Powell, 1995)							
SiO_2	Al_2O_3	CaO	MgO	FeO	K_2O	Na_2O	
71.03	16.01	1.24	1.74	4.87	3.08	2.02	
(b) Mole per cent [converted from (a)]							
SiO_2	Al_2O_3	CaO	MgO	FeO	K_2O	Na_2O	
76.89	10.21	1.44	2.81	4.41	2.12	2.12	
(c) PERMIAN BULK (permpg3) [after subtracting 2 mol.% ksp with K_2O (0.9) and Na_2O (0.1) and normalizing]							
SiO_2	Al_2O_3	CaO	MgO	FeO	K_2O	Na_2O	
76.93	10.16	1.47	2.87	4.50	1.94	2.14	
(d) Calculated mineral compositions and modes at 655 °C and 6.5 kbar using (c)							
x(bi)	y(bi)	x(mu)	y(mu)	x(g)	z(g)	ca(pl)	k(pl)
0.522	0.430	0.478	0.950	0.835	0.051	0.252	0.014
bi	mu	g	pl	q	sill		
14.60	12.36	4.97	20.67	45.30	2.11		
(e) EO-ALPINE BULK (eopg3)							
H_2O	SiO_2	Al_2O_3	CaO	MgO	FeO	K_2O	Na_2O
3.35	77.17	8.55	1.46	2.69	2.93	1.62	2.22

Correction of K-feldspar is done by the subtraction of a proportion (2%) of ksp-molecules (*ksp*) from the bulk composition (line c). This subtraction is done on a one oxide basis, i.e. K-feldspar consisting of the four oxides: $3SiO_2 + 0.5Al_2O_3$ and 0.5 ($K_2O + Na_2O$) – is here written as: *ksp* = 3/4 SiO_2, 0.5/4 Al_2O_3 0.45/4 K_2O and 0.05/4 Na_2O. The total proportion of K-feldspar in the rock, *pksp* (here volumetrically *pksp* = 2%~molar2% as the molar volumes of most minerals are similar), is then simply subtracted from bulk *m* (e.g. that in line c). This is done for each oxide separately. As the sum of all oxides in the bulk and in feldspar are both written on a one oxide basis, the result is only part of one oxide, namely 1 - *pksp*. Thus, the result then only needs to be normalized by (1 - *pksp*) so that the sum of the oxides in the corrected bulk *m*1 is again 100% (i.e. line e). In short, the procedure to arrive at line d from line c is simply: $m1 = (m - pksp * ksp)/(1 - pksp)$.

Table 4. Average *P–T* and average *P* calculations performed with THERMOCALC 3.23 and the mineral compositions published by Habler & Thöni (2001).

AX (http://www.esc.cam.ac.uk/astaff/holland/) gives the following end-member activities
mu = 0.74
cel = 0.0147
fcel = 0.016
phl = 0.0281
ann = 0.048
east = 0.034
py = 0.00112
gr = 0.0014
alm = 0.32
an = 0.48
ab = 0.67
Average *PT* gives
$T = 623 \pm 191$ °C; $P = 7.3 \pm 2.80$ kbar
Average *P* gives
$P = 5.9 \pm 0.90$ kbar at 600 °C
$P = 6.2 \pm 0.92$ kbar at 625 °C
$P = 6.4 \pm 0.95$ kbar at 650 °C
$P = 6.6 \pm 0.97$ kbar at 675 °C
Uncertainties are at 2σ level; σ_{fit} passes the χ^2 test.

(Fig. 2e). This is in fact the case (compare Fig. 2d,e with biotite of DFG in Table 1: they are both near $X_{Fe} = 0.57$). Whereas the metamorphism was assumed to be H_2O-saturated during the Permian event, the H_2O content of the bulk composition during the Eo-Alpine event is assumed to be provided by the Permian mineral assemblage that is reworked then. The consequence of the chosen proportions of the minerals excluded from the bulk composition is discussed below.

The pseudosections and their robustness

For the bulk compositions derived above ('permpg3' for the Permian and 'eopg3' for the Eo-Alpine of Tables 2 & 3) we have calculated *P–T* and $T–M_{H_2O}$ pseudosections and use them to derive information on the evolution and content of water in these rocks. As these pseudosections form the basis of all subsequent discussion and because 'eopg3' is a direct derivative of 'permpg3', it is important to discuss the pseudosection for 'permpg3' and its robustness.

A *P–T* pseudosection for 'permpg3' was drawn for staurolite, garnet, paragonite, chlorite, muscovite, aluminosilicate, biotite, plagioclase, K-feldspar, quartz, water and melt in the system NCKFMASH (Fig. 3a). If no metamorphic event preceded the Permian it is reasonable to suppose that the precursor rocks were water-saturated sediments: the pseudosection was constructed with water 'in excess' for the consideration of the prograde path (Guiraud *et al.*, 2001). The pseudosection was constructed using the software THERMOCALC 3.23 (Powell *et al.*, 1998, and upgrades), using the thermodynamic data set of Holland & Powell (1998), the 5.5 upgrade of Nov. 2003). The pseudosection was contoured for the water content (defined as the percentage of the crystallographically bound H_2O of the solid phase assemblage) normalized to the H_2O content (mol.%) of the most hydrated assemblage in the *P–T* region considered (Guiraud *et al.*, 2001). For the pseudosection shown in Fig. 3a this most-hydrated assemblage is bi + mu + chl (+ pl + q + H_2O) at 550 °C and 6 kbar.

Chemical composition contours were added to the pseudosection in order to constrain the correct *P–T* conditions of our equilibrium assemblage within individual reaction spaces (Fig. 3b). In particular, the diagram was contoured for X_{Fe} in garnet, X_{Fe} in biotite and X_{An} in plagioclase (called x(g); x(bi) and ca(pl) in Fig. 3b, respectively) in the stability field of the peak assemblage and the lower-*T* adjacent assemblage g + bi + mu + st (+ pl + q + H_2O). The X_{Fe} in garnet increases with a pressure decrease by 1 kbar (7–6 kbar) from around 0.83 until 0.87 at the lower stability of the peak assemblage g + bi + mu + sill (+ H_2O + q + pl). Similarly, the contours for X_{Fe} in biotite increases from 0.5 to 0.57 with a pressure decrease of *c.* 1 kbar. The X_{An} in plagioclase shows a minor increase from 0.250 to 0.256 over the same pressure decrease.

In order to check the robustness of the pseudosection towards changes in the bulk composition two approaches are followed. First, the trivariant fields of interest (i.e. in the vicinity of the Permian metamorphic peak) for a number of bulk compositions of other rocks from the Koralpe region have been calculated with similar peak assemblages and for the different approaches. This is shown in Fig. 3(c). It may be seen that the trivariant fields g + bi + mu + sill (+ pl + q + H_2O) and g + bi + mu + ky (+ pl + q + H_2O) have a quite robust position in *P–T* for the bulk compositional variation shown in Table 2.

Second, we have checked for changes of the pseudosection with a systematic variation of Al, and Fe by comparing our result with *T–X* sections published by White *et al.* (2001). White *et al.* (2001) showed in their figs 7 and 8 the changes that pseudosections for 'normal' pelitic bulk compositions will undergo for changes in $X_{Fe} = Fe/(Fe + Mg)$ and $X_{Al} = Al/(Al + Fe + Mg)$. It may be seen that their *T–X* section corresponds to the pseudosection shown in Fig. 3 at the corresponding *P* and *T* and that there is little change in the topology of the phase diagram for several tens of relative per cent in Al and Fe variation. The pseudosections calculated here are therefore quite robust towards errors in our estimates of the bulk composition.

THE PERMIAN EVOLUTION

The pseudosection in Fig. 3(a) shows that the solidus for this bulk composition is roughly isothermal in the pressure range considered: from 4 to 9 kbar it varies between ~650 and 670 °C. For lower-grade rocks below ~600 °C and above ~5 kbar the diagram predicts the equilibrium assemblage g + bi + mu + chl (+ pl + q + H_2O). Importantly, the pseudosection predicts a trivariant paragenesis corresponding to the Per-

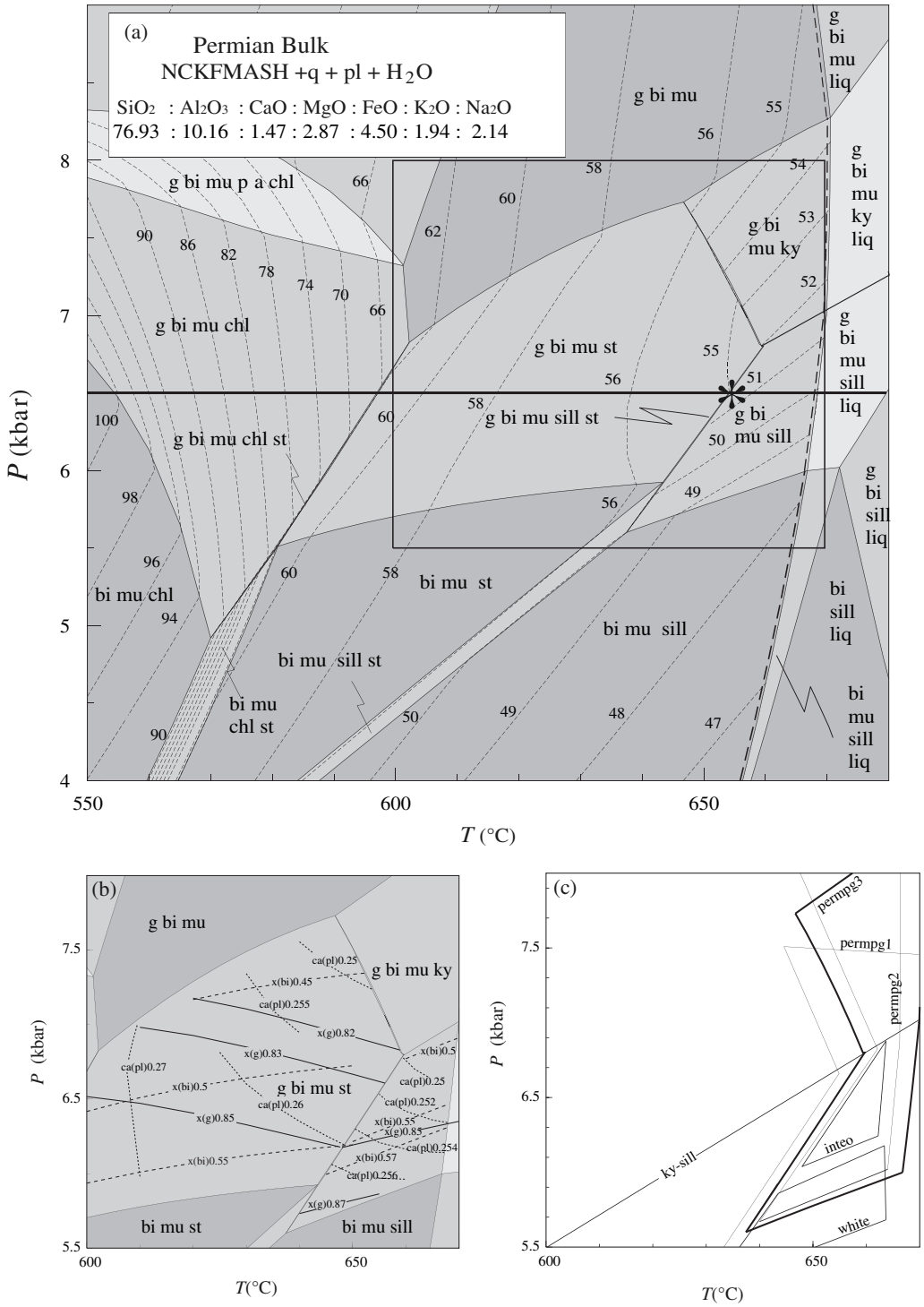

Fig. 3. *P–T* pseudosection for the Permian bulk composition of the Plattengneiss assuming H_2O, q and pl in excess. (a) The bulk composition used is that of 'permpg3' from Table 2. The asterisk at 6.5 kbar and *c*. 650 °C marks the peak conditions suggested for the Permian using the mineral compositions of Habler & Thöni (2001) and THERMOCALC 3.23. The thick black line at 6.5 kbar marks the section position of Fig. 4(a). Thick dashed line is the solidus. The diagram is contoured (with thin dashed lines) for water content of the mineral assemblages, normalized to the most hydrated assemblage (at 550 °C and 6 kbar). These water mode contours continue across the solidus, but they are not shown there. The rectangular box indicates the *P–T* range of the diagrams in (b) and (c). (b) Section from the diagram in (a) showing some contours for calculated mineral chemical parameters in the phase fields g + bi + mu + sill and g + bi + mu + st. Abbreviations are: x(bi) = X_{Fe} of biotite; x(g) = X_{Fe} of garnet; ca(pl) = X_{An} of plagioclase. (c) Diagram showing the variability of the trivariant field g + bi + mu + aluminosilicate as a function of bulk composition. The outline of this phase field is shown for all bulk compositions listed in Table 2. Thick line marks the bulk composition 'permpg3' used throughout this study.

mian peak assemblage of the Plattengneiss in a field below the solidus (near asterisk in Fig. 3). It may be seen that this peak assemblage contains only *c.* 50% of the water content in the minerals compared with the low-grade assemblage. A comparison with Table 1 shows that the computed mineral parameters of the peak assemblage in the diagram (Fig. 3b) fit extremely well with the measured Permian mineral chemistry from the Kor- and Saualpe at ~6 kbar and 650 °C. These *P–T* conditions are the most reliable ones for the Permian peak compared with the results shown in Table 4 or the ones by Habler & Thöni (2001), that slightly over- or underestimate the metamorphic conditions.

In order to discuss the evolution of water content during the Permian event on this pseudosection, a *P–T* path is needed. Schuster *et al.* (2001) suggested that much of the Permian evolution occurred isobarically. Assuming an isobaric heating and cooling path at 6.5 kbar, the evolution of the water content is considered on a diagram where M_{H_2O} (in mol.%) is plotted against temperature at constant pressure of 6.5 kbar as indicated by the thick isobaric line in Fig. 3(a) (fig. 4a). Prograde dehydration during isobaric heating results in water loss and a path in Fig. 4(a) that tracks along the water saturation line, because only a small proportion of free water is likely to remain along grain boundaries (Guiraud *et al.*, 2001). Garnet is first formed below the *P–T* range considered, in paragonite and later chlorite and staurolite-bearing assemblages. On traversing a series of phase fields with progressive dehydration, ultimately the peak assemblage g + bi + mu + sill (+ pl + q + H_2O) forms at ~650 °C when staurolite is lost. Onset of cooling will 'freeze' the water content of the assemblage to that of the metamorphic peak as the remaining free fluid is used up with incipient re-hydration. As such, the water content of the rocks at the end of the Permian event is likely to have been just below 4 mol.% H_2O at these conditions. Subsequent cooling will preserve this water content (shaded arrow in Fig. 4a) and also the peak assemblage, although it is possible that kyanite may grow at the expense of sillimanite. Note that the entire post peak evolution evolves very close to the staurolite out line. Thus it is possible throughout that some rocks preserve Permian staurolite – as they do in more hydrated, but otherwise compositionally similar rocks outside the Plattengneiss shear zone.

THE EO-ALPINE EVOLUTION

The water content of the Plattengneiss at the end of the Permian metamorphic cycle is not necessarily the same as that at the start of the Eo-Alpine cycle. Re-hydration of the Plattengneiss may have occurred between the two events. In order to assess this possibility a T–M_{H_2O} pseudosection was calculated that corresponds to Fig. 4(a), but using a bulk composition that is appropriate for the Eo-Alpine as derived above. Figure 4(b) shows this T–M_{H_2O} pseudosection for 14 kbar. This diagram is not quite appropriate to illustrate the entire heating path during the Eo-Alpine event because much of this may have occurred at pressures different from 14 kbar. Nevertheless, the diagram can be used to illustrate the near-peak prograde evolution during the Eo-Alpine.

Figure 4(b) shows that the assemblage at 700 °C and 14 kbar is g + bi + mu + (pl + q) (as marked by the asterisk), corresponds to the Eo-Alpine peak assemblage of sample 48/92 from which this bulk composition was derived. In Fig. 4(b), this paragenesis is water undersaturated and is stable for a relatively narrow range of water content between $M_{H_2O} = 3.0$ and $M_{H_2O} = 3.5$ mol.%; Fig. 4b). At somewhat higher water contents, melting commences. At lower water contents, kyanite and/or K-feldspar become stable. When kyanite occurs, Fig. 4(b) predicts that its mode should decrease towards the Eo-Alpine peak consistent with the observation that kyanite often has started to be consumed along its margins and replaced by white mica. For the subsequent discussion we use $M_{H_2O} = 3.35$ mol.% in the centre of the suggested water content range.

The fact that this water content is slightly below the water mode suggested for the end of the Permian cycle (M_{H_2O} about 4 mol.%, Fig. 4a) is because some of the hydrous mineral muscovite was removed from the bulk composition. Taking this into account, the rocks are consistent with a lack of hydration (or dehydration) between the Permian and the Eo-Alpine, remaining closed system. Varying the proportions of the removed minerals changes not only the water content but the remainder of the bulk composition used in the calculation of Fig. 4(b). Recalculation of the figure at 14 kbar shows that varying the proportion of Permian muscovite that is removed in order to get the Eo-Alpine white mica proportion, from 0 (all muscovite are Permian fish), to 0.75 (leaving some muscovite to be Permian fish), would shift the solidus temperature from 750 to 730 °C, and would decrease the temperature of the upper temperature boundary of kyanite stability from 610 to 600 °C. Removal of lesser proportions of garnet and/or K-feldspar has a smaller effect on the phase relationships. This shows that the assumptions made in generating the Eo-Alpine bulk composition from the Permian bulk composition are not controlling our main conclusion: that the Eoalpine event occurred at a constant water content that was established at the end of the Permian event.

P–T diagram for the Plattengenesis

A *P–T* pseudosection for the Plattengneiss can now be constructed with a bulk composition for which the water content is known (Fig. 5). As such, this pseudosection is a considerable improvement on the results presented by Stüwe & Powell (1995). Figure 5 shows that the solidus has a positive slope rising from 660 °C at 6 kbar to 750 °C at 16 kbar. Above ~7 kbar, the solidus is water undersaturated. For the chosen H_2O

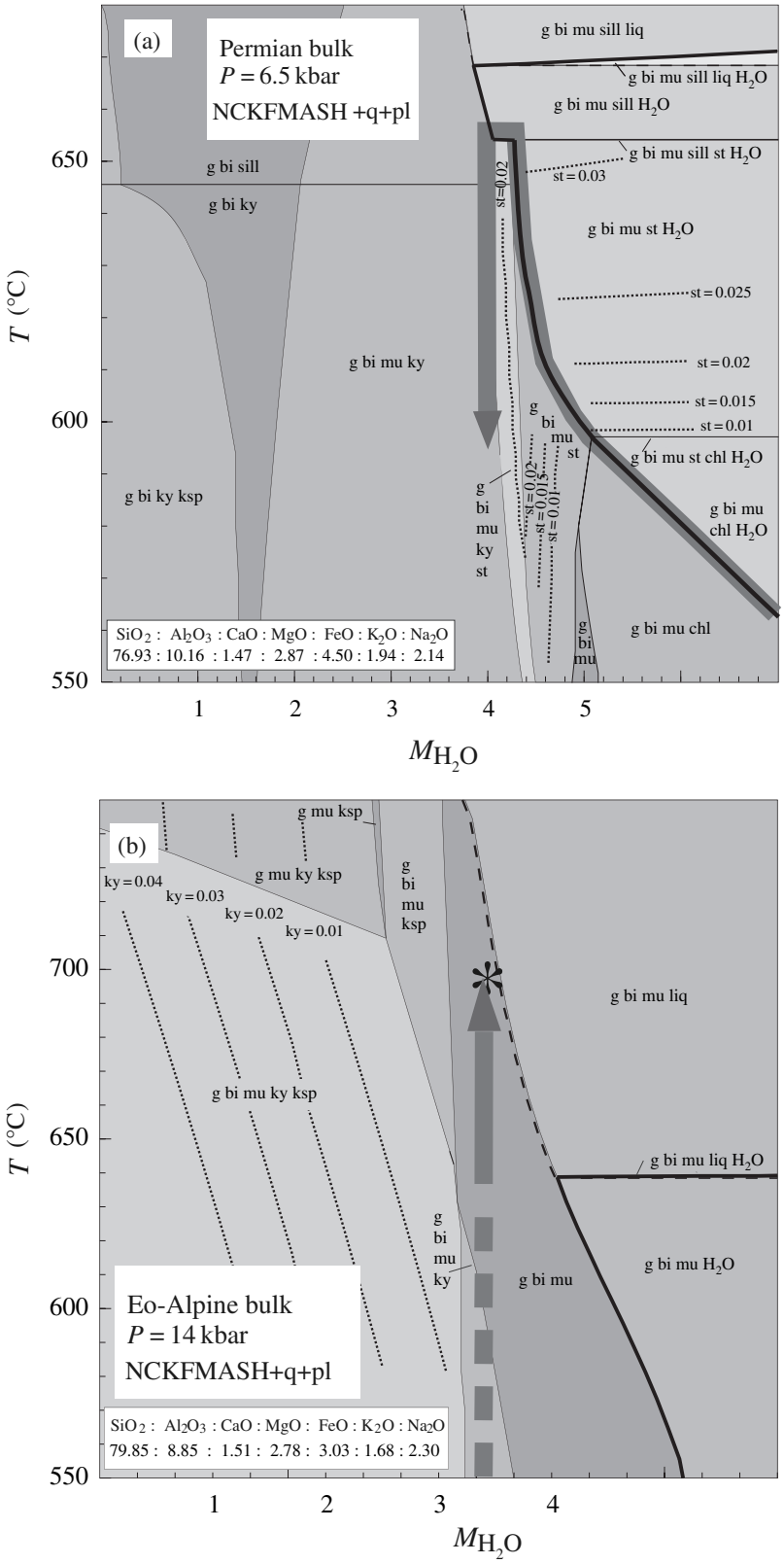

Fig. 4. T–M_{H_2O} pseudosections for (a) the Permian bulk composition and (b) the Eo-Alpine bulk composition. On both diagrams the M_{H_2O} axis is labelled in mol.% H_2O in the bulk rock; the thick solid line marks the water saturation line and the thick dashed line is the solidus. Mode contours for staurolite (abbreviated with st) are shown in the st-bearing fields. (a) The diagram for the Permian prograde path at 6.5 kbar. This diagram is a section along the thick line shown in Fig. 3(a) at 6.5 kbar. However, note that maximum water mode used here is not sufficient to saturate the entire diagram with water. Thus, there are minor differences to Fig. 3(a) at very high and very low temperatures. The thick shaded arrow marks the prograde path suggested for the Permian evolution of the Plattengneiss. (b) T–M_{H_2O} pseudosection for the Eo-Alpine bulk composition constructed at 14 kbar. The bulk composition shown in the inset is that of Table 3 line e without H_2O and normalized to 100%. The shaded arrow marks the prograde path during the Eo-Alpine. It is dashed at low temperature because it is likely to have evolved at pressures different from 14 kbar in this region. Mode contours for kyanite (abbreviated with ky) are shown in the kyanite bearing fields.

content, water-saturated parageneses are predicted only in a small region below 7 kbar and between 640 and 670 °C. The pseudosection predicts both the peak parageneses of the Plattengneiss at the peak conditions around 14 kbar and 700 °C and the Permian retrograde assemblage g + bi + mu + ky (+ pl + q)

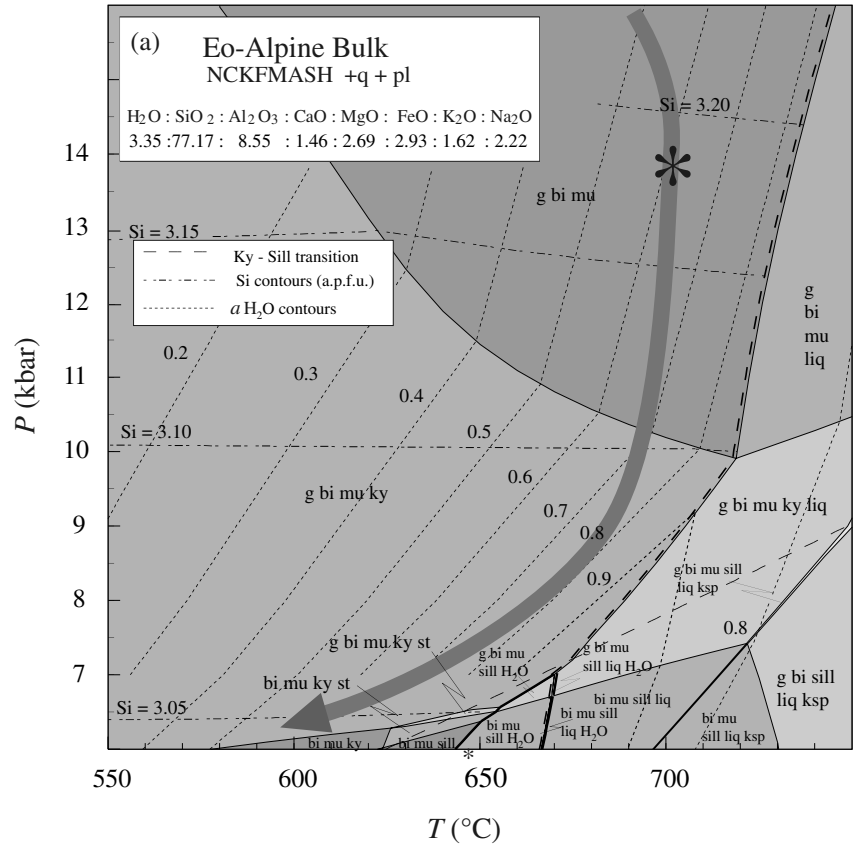

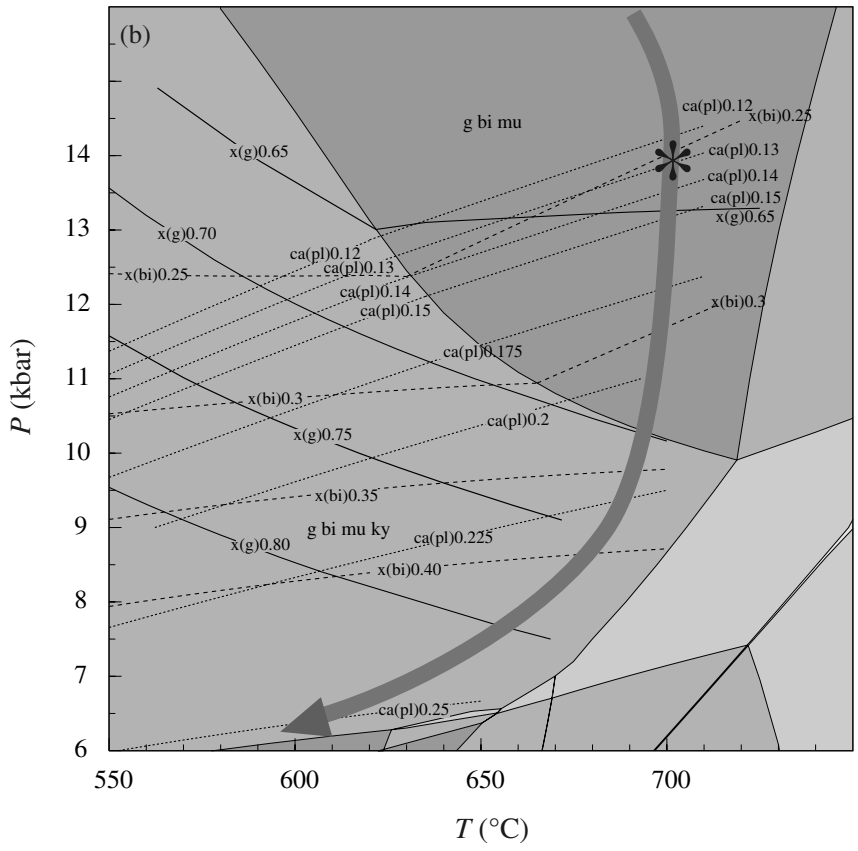

Fig. 5. *P–T* pseudosection for the Eo-Alpine bulk composition of the Plattengneiss using the H_2O content suggested by Fig. 4(b). The Eo-Alpine metamorphic peak conditions are marked by the asterisk. The thick solid line marks the water saturation line. The thick dashed line is the solidus. (a) The diagram is contoured for water activity and Si-content of muscovite of the equilibrium assemblages. The thick shaded arrow is the *P–T* path is that suggested by Thöni (1999). (b) The same diagram contoured for some mineral chemical parameters (as explained in Fig. 3b).

with or without staurolite. The upper pressure limit of biotite is above 16 kbar. Water activity contours on this pseudosection show that the Eo-Alpine metamorphic peak is characterized by a water activity around 0.6. The contours furthermore show that $a(H_2O)$ increases in both fields with moderate temperature increase but drastic pressure decrease. The Si-content of muscovite (for a 12 oxygen formula unit) is also contoured and matches the suggested formation conditions for the Eo-Alpine-formed white mica (Si-content = 3.15–3.25; Tenczer & Stüwe, 2003).

Comparably to the Permian diagram in Fig. 3(b), Fig. 5(a) is also contoured for X_{Fe} in garnet, X_{Fe} in biotite and X_{An} in plagioclase in the P–T range of interest in Fig. 5(b). Table 1 shows the relevant measured mineral chemistry for comparison. The X_{An} of the diagram matches well with the actually measured values of 0.13–0.14 at Eo-Alpine peak conditions around 14 kbar and 700 °C. At these conditions the diagram predicts X_{Fe} in biotite to be 0.25 and X_{Fe} in garnet of *c.* 0.65. The actual values in the rocks however are slightly higher (X_{Fe} in biotite is typically 0.3; X_{Fe} in garnet is 0.7) than the computed ones. This could mean that the actual values of X_{Fe} in garnet and biotite seem to be slightly influenced by retrograde metamorphism along the decompression path around 10–12 kbar.

DISCUSSION AND CONCLUSIONS

We conclude that the Permian prograde path led to metamorphic peak conditions around 650 °C and 6–6.5 kbar with the rocks having progressively dehydrated through to the peak. The mineral assemblages developed in the Eo-Alpine event are consistent with the rocks being a closed system with respect to H_2O following this Permian event, with a metamorphic peak around 14 kbar and 700 °C when the Plattengneiss developed its characteristic form. This is likely to have been followed by substantial isothermal decompression before final cooling. This interpretation is directly inferred from the slope of the $a(H_2O)$ contours on Fig. 5(a) and indirectly supported by more hydrated rocks of otherwise similar bulk composition above and below the Plattengneiss shear zone. These rocks typically contain staurolite, paragonite and/or chlorite; phases that appear for the same path at somewhat more hydrated conditions in Fig. 4.

The Eo-Alpine evolution of the Plattengneiss was water-undersaturated assuming a constant water-content nature of the study area. Therefore, the incomplete equilibration of the Plattengneiss can be explained by the absence of a fluid phase – even at temperatures of 700 °C. This conclusion can be placed in a wider context: the fact that the Plattengneiss did equilibrate partially at all can be attributed to the intense deformation it experienced and the recrystallization that resulted from it.

The evolution of water content and $a(H_2O)$ of the Plattengneiss from the Permian to the present is summarized in Fig. 6. The key feature of this is the decrease of water content during the Permian event which is drawn schematically for the prograde Permian evolution. This prograde dewatering terminated at the metamorphic temperature peak where we established a water content around M_{H_2O} = 3–4 mol.%. As all this water is crystallographically bound (and is substantially less than what is required to saturate the rocks during the entire subsequent evolution), we infer that this water content remained constant from then onwards to the present day. This is confirmed by Fig. 4 which showed that comparable water contents in both Permian and Eo-Alpine bulks produce the corresponding peak parageneses. Once water-undersaturated conditions are established (Powell *et al.*, 2005) and the water content remains constant, the activity $a(H_2O)$ is a passive variable to the water content. In fact, $a(H_2O)$ only has meaning when a mineral assemblage can be considered to be equilibrating. Then the $a(H_2O)$ is a consequence of the mineral assemblage and P–T conditions, at a specified water content.

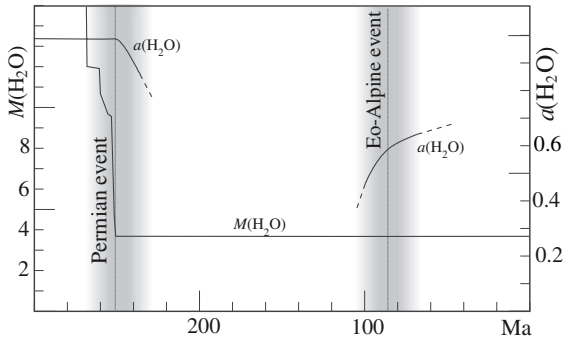

Fig. 6. Cartoon summarizing the suggested evolution of water activity and water content of the Plattengneiss from the Permian to the present. Note that the water activity line cannot be connected between the two events because it is only defined while the rocks are equilibrating.

The calculations presented here also confirm the Eo-Alpine P–T path suggested by Thöni (1999). The retrograde part of this path is shown as the thick arrow superimposed in Fig. 5. Thöni (1999) suggested that burial of the Plattengneiss occurred at low temperature up to *c.* 20 kbar and was followed by isobaric heating from 500 °C to above 600 °C, followed by near isothermal decompression reaching the thermal peak at *c.* 14 kbar. This arrival at the peak from higher pressure was also suggested by Stüwe & Powell (1995), Gregurek *et al.* (1997) and Thöni & Jagoutz (1992). Tenczer & Stüwe (2003) have shown that lower-grade rocks have higher water activities. This is consistent with a substantial post peak decompression phase: Figure 5(a) shows that drastic post peak decompression leads to higher water activities at lower grade. On the other hand, if cooling accompanied decompression, the water activity should remain constant or decrease.

Partial melting of the Plattengneiss is a conceivable process during further decompression after the peak, given the phase relationships in Fig. 5. Heede (1997) has described pegmatoids spatially associated with eclogites that cross-cut the regional fabric and that may have been related to the late Eo-Alpine evolution. Slightly higher water contents than those used to calculate Fig. 5 would shift the solidus towards lower temperatures (compare with higher water content phase fields on Fig. 4b) causing the solidus to be intersected by an essentially isothermal post-peak decompression part of the *P–T* path.

Concerning the tectonic evolution of the Plattengneiss prior to the Eo-Alpine event, it remains unclear if the rocks were exhumed to the surface after the Permian event or remained buried at depth. Evidence of Permo-Mesozoic sediments in the Austroalpine nappe suggests that at least some parts of this complex were fully exhumed after the Permian event. Here, we have shown that the water content of the rocks at the end of the Permian was the same as that at the start of the Eo-Alpine evolution. This indicates that no hydration of the rocks occurred between the two events, which may possibly indicate that the rocks were not completely exhumed to the surface where they may have experienced re-hydration by meteoric waters.

ACKNOWLEDGEMENTS

This project was supported by the FWF grant P-12846 and P-15474. RP acknowledges support of ARC DP 0451770. We thank J. Dale, G. Habler and R. White for discussions. G. Habler and M. Guiraud are also thanked for their constructive comments during the formal review of this manuscript.

REFERENCES

Berman, R. G., 1988. Internally consistent thermodynamic data for minerals in the system Na_2O–K_2O–CaO–MgO–FeO–Fe_2O_3–Al_2O_3–SiO_2–TiO_2–H_2O–CO_2. *Journal of Petrology*, **29,** 445–522.

Brown, T. H., Berman, R. G. & Perkins, E. H., 1988. GEO-CALC: software package for calculation of pressure–temperature–composition phase diagrams using an IBM or compatible personal computer. *Computers and Geoscience*, **14,** 279–289.

Ehlers, K., Stüwe, K., Powell, R., Sandiford, M. & Frank, W., 1994. Thermometrically inferred cooling rates from the Plattengneis, Koralm region, Eastern Alps. *Earth and Planetary Science Letters*, **125,** 307–321.

Franceschelli, M., Eltrudis, A., Memmi, I., Palmeri, R. & Carcangiu, G., 1998. Multi-stage metamorphic re-equilibration in eclogitic rocks from the Hercynian basement of NE Sardinia (Italy). *Mineralogy and Petrology*, **62,** 167–193.

Frank, W., Esterlus, M., Frey, I., Jung, G., Krohe, A. & Weber, J., 1983. Die Entwicklungs- geschichte von Stub- und Koralpenkristallin und die Beziehung zum Grazer Paläozoikum. *Hochschulschwerpunkt*, **S15,** 263–293.

Frey, M., Desmons, J. & Neubauer, F., 1999. The new metamorphic map of the Alps. *Schweizerische Mineralogische und Petrographische Mitteilungen*, **79,** 1–4.

Gregurek, D., Abart, R. & Hoinkes, G., 1997. Contrasting eoalpine *P–T* evolutions in the southern Koralpe, Eastern Alps. *Mineralogy and Petrology*, **60,** 61–80.

Guiraud, M., Powell, R. & Rebay, G., 2001. H_2O in metamorphism and unexpected behaviour in the preservation of metamorphic mineral assemblages. *Journal of Metamorphic Geology*, **19,** 445–454.

Habler, G. & Thöni, M., 2001. Preservation of Permo-Triassic low-pressure assemblages in the Cretaceous high-pressure metamorphic Saualpe crystalline basement (Eastern Alps, Austria). *Journal of Metamorphic Geology*, **19,** 679–697.

Heede, H. U., 1997. Isotopengeologische Untersuchungen an Gesteinen des ostalpinen Saualpenkristallins, Kärnten-Österreich. *Münstersche Forschungen zur Geologie und Paläontologie*, **81,** 1–168.

Hejl, E., 1997. Cold spots during the Cenozoic evolution of the Eastern Alps: thermo-chronological interpretation of apatite fission-track data. *Tectonophysics*, **272,** 159–173.

Holland, T. J. B. & Powell, R., 1998. An internally consistent thermodynamic data set for phases of petrological interest. *Journal of Metamorphic Geology*, **16,** 309–343.

Krohe, A., 1987. Kinematics of Creatceaous nappe tectonics in the Austroalpine basement of the Koralpe region (eastern Austria). *Tectonophysics*, **136,** 171–196.

Kurz, W., Fritz, H., Tenczer, V. & Unzog, W., 2002. Tectono-metamorphic evolution of the Koralm Complex (Eastern Alps): constraints from microstructures and textures of the 'Plattengneis' shear zone. *Journal of Structural Geology*, **24,** 1957–1970.

Lister, G. S., Forster, M. A. & Rawling, T. J., 2001. Episodicity during orogenesis. *Geological Society Special Publication*, **184,** 89–113.

Miller, C. & Thöni, M., 1997. Eo-Alpine eclogitisation of Permian MORB-type gabbros in the Koralpe (Eastern Alps, Austria): new geochronological, geochemical and petrological data. *Chemical Geology*, **137,** 283–310.

Morauf, W., 1981. Rb-Sr- und K-Ar-Isotopen-Alter an Pegmatiten aus Kor- und Saualpe, SE-Ostalpen, Österreich. Rb/Sr and K/Ar isotope dating of the pegmatites of Koralpe and Saualpe, southeastern Eastern Alps, Austria. *Tschermaks Mineralogische und Petrographische Mitteilungen*, **28,** 113–129.

Neubauer, F., Dallmeyer, R. D., Dunkl, I. & Schirnik, D., 1995. Late Cretaceous exhumation of the metamorphic Gleinalm dome, Eastern Alps: kinematics, cooling history and sedimentary response in a sinistral wrench corridor. *Tectonophysics*, **242,** 79–98.

Oberhänsli, R., Bousquet, R., Engi, M. *et al.*, 2004. *Metamorphic Structure of the Alps (1:1 000 000)*. Commission for the Geological Map of the World (UNESCO), Paris.

Powell, R., Holland, T. J. B. & Worley, B., 1998. Calculating phase diagrams involving solid solutions via non-linear equations, with examples using THERMOCALC. *Journal of Metamorphic Geology*, **16,** 577–588.

Powell, R., Guiraud, M. & White, R. W., 2005. Truth and beauty in metamorphic mineral equilibria: conjugate variables and phase diagrams. *Canadian Mineralogist*, **43,** 21–33.

Putz, M., Stüwe, K., Jessell, M. & Calcagno, P., 2006. Three-dimensional model and late stage warping of the Plattengneis Shear Zone in the Eastern Alps. *Tectonophysics*, **412**: 87–103.

Rickers, K., Raith, M. & Dasgupta, S., 2001. Multistage reaction textures in xenolithic high-Mg-Al granulites at Anakapalle, Eastern Ghats Belt, India; examples of contact polymetamorphism and infiltration-driven metasomatism. *Journal of Metamorphic Geology*, **19,** 561–580.

Schuster, R., Scharbert, S., Abart, R. & Frank, W., 2001. Permo-Triassic extension and related HT/LP metamorphism in the Austroalpine-Southalpine realm. *Mitteilungen der Gesellschaft der Geologie- und Bergbaustudenten*, **45,** 111–141.

Stüwe, K., 1998. Heat sources of Cretaceous metamorphism in the Eastern Alps – a discussion. *Tectonophysics*, **287,** 251–269.

Stüwe, K. & Ehlers, K., 1996. The qualitative zoning record of minerals. A method for determining the duration of metamorphic events? *Mineralogy and Petrology*, **56,** 171–184.

Stüwe, K. & Powell, R., 1995. PT paths from modal proportions: application to the Koralm Complex, Eastern Alps. *Contributions to Mineralogy and Petrology*, **119,** 83–93.

Tenczer, V. & Stüwe, K., 2003. The metamorphic field gradient in the eclogite type locality, Koralpe region, Eastern Alps. *Journal of Metamorphic Geology*, **21,** 377–393.

Thöni, M., 1999. A review of geochronological data from the Eastern Alps. *Schweizerische Mineralogische und Petrographische Mitteilungen*, **79,** 209–230.

Thöni, M., 2002. Sm–Nd isotope systematics in garnet from different lithologies (Eastern Alps); age results, and an evaluation of potential problems for garnet Sm–Nd chronometry. *Chemical Geology*, **185,** 255–281.

Thöni, M. & Jagoutz, E., 1992. Some new aspects of dating eclogites in orogenic belts: Sm–Nd, Rb–Sr, and Pb–Pb isotopic results from the Austroalpine Saualpe and Koralpe type-locality (Carinthia/Styria, southeastern Austria). *Geochimica et Cosmochimica Acta*, **56,** 347–368.

Thöni, M. & Miller, C., 1996. Garnet Sm–Nd data from the Saualpe and the Koralpe (Eastern Alps, Austria): chronological and *P–T* constraints on the thermal and tectonic history. *Journal of Metamorphic Geology*, **14,** 453–466.

White, R. W., Powell, R. & Holland, T. J. B., 2001. Calculation of partial melting equilibria in the system Na_2O–CaO–K_2O–FeO–MgO–Al_2O_3–SiO_2–H_2O (NCKFMASH). *Journal of Metamorphic Geology*, **19,** 139–153.

Zeck, H. P. & Whitehouse, M. J., 2002. Repeated age resetting in zircons from Hercynian-Alpine polymetamorphic schists (Betic-Rif tectonic belt, S. Spain); a U–Th–Pb ion microprobe study. *Chemical Geology*, **182,** 275–292.

Received 1 August 2005; revision accepted 9 February 2006.